Preliminary design of a retrofitted ultralight aircraft with a hybrid electric fuel cell power system

Preliminary design of a retrofitted ultralight aircraft with a hybrid electric fuel cell power system

Teresa Donateo[1*], Antonio Ficarella[1], Leonardo Lecce[2]

[1] University of Salento, va per Monteroni, 73100, Lecce, ITALY
[2] Novotech Aerospace Advanced Technology srl, Strada Provinciale 143 KM. 2 74020 Avetrana (TA), Italy

[*]Corresponding author: teresa.donateo@unisalento.it

Abstract. Emission-free aerial propulsion can be achieved with a proton-exchange membrane fuel cell (PEM-FC). In the present investigation, this potential is addressed by designing a hybrid electric power system with fuel cells for an ultralight aerial vehicle to be retrofitted from a conventional fossil-fuelled piston engine configuration. The proposed power system includes a fuel cell, a lithium battery, and a compressed hydrogen vessel. A procedure is proposed to find the size of these components that minimizes the total mass and satisfies the target of a size below 200L and uses performance data of commercially available components. A comparison of different energy management approaches, with and without on-board charge of the battery, is performed. The results underline that the optimal solution is to select the size of the fuel cell to meet the cruise electric request and point out that the maximum discharge current of the battery must be regarded as a key issue in sizing this component, because of the very high take-off power.

1. Introduction

Hydrogen power systems are one of the main development prospects of our century in all means of transportation. Among them, the conversion of hydrogen energy in a fuel cell system guarantees the highest value of efficiency. The use of hydrogen in fuel cells has the potential to achieve zero emissions but requires innovation, research, and investment [1].

Batteries or other electric storage systems are usually coupled with the fuel cell in a hybrid electric architecture to overcome its limitations([3], [4]. A compressed or liquified hydrogen vessel has higher gravimetric energy density but lower volumetric energy density than lithium batteries, while the fuel cell has a low power density compared with the battery [5]. The role of the battery in a fuel cell system is also to overcome the slower dynamic response of the fuel cell. More than ten seconds may elapse from giving a command to reaching the desired power [3]. Hybridization, on the other hand, requires efficient energy management strategies and a careful consideration of operating conditions and technological limits.

Methodologies for the preliminary design of hybrid electric power systems with fuel cells were proposed in the scientific literature for aircraft ranging from small Unmanned Aerial Vehicles (UAV) to regional aviation. Sizing a fuel cell system for ultralight aviation is not a trivial task because there are several key factors to consider [6]. The size of the fuel cell is often arbitrarily selected [3] or put equal to the cruise power in a single specific mission [7]. Some studies propose an optimization of the fuel

cell system using as a metric the hydrogen fuel consumption and the total mass [8][9]. Reducing the weight of the fuel cell system, inclusive of the hydrogen vessel, is indeed crucial for optimizing the performance of an ultralight aircraft. However, as pointed out in [10], the volumetric energy density is of equal importance in the aerospace field [11]. Analytic Hierarchy Process was used in [2] to evaluate the most suitable fuel cell type for integration into a small aircraft hybrid powertrain, with proton exchange membrane (PEM) fuel cells being found to be the best suited. A modular multi-stack system consisting of four 140kW stacks arranged in parallel was proposed by Abu Kasim et al. [12] for the retrofitting of a Cessna aircraft.

The present investigation proposes a methodology for the sizing of the three main components of a hydrogen hybrid electric architecture: the PEM fuel cell system, the battery, and the hydrogen vessel. The fuel cell system is characterized in terms of power-to-weight and power-to-volume indexes, while the gravimetric and energy stored on board depend on the hydrogen storage system. Another novelty of this investigation is the usage of values of energy and power densities derived from commercial datasheets for the sizing of the power system.

2. The SERENA project

The goal of the project is the development of zero-emission propulsion architectures for General Aviation by retrofitting the Novotech Seagull. The Seagull aircraft is a high-wing amphibian aircraft with two seats, equipped with a single piston engine. The main specifications are reported in Figure 1.

Property	*Value*
Wingspan	10.5 m
Wing area	13.5 m^2
Max Gross Weight	700kg
Maximum Zero Fuel Weight	650 kg
Maximum Baggage Weight	20 kg
Pay weight	80kg
Power Loading	6.5 kg/HP
Engine type	Rotax 912 ULS2
Engine power	100hp @ 5800rpm
Fuel tank capacity	70 L (50kg)

Figure 1. Picture and main specifications of the Seagull

The "zero-emission" configuration was obtained by considering a hybrid electric propulsion system with a PEM fuel cell. It is worth noting that the proposed powertrain is a "zero-emission" if we consider the emissions produced during the usage and neglect the environmental impact of the water produced by the chemical reaction taking place in the fuel cell. The indirect environmental impact of the proposed power system depends on the emission intensity of the electricity generation system (for the charge of the battery) and the hydrogen production process [13].

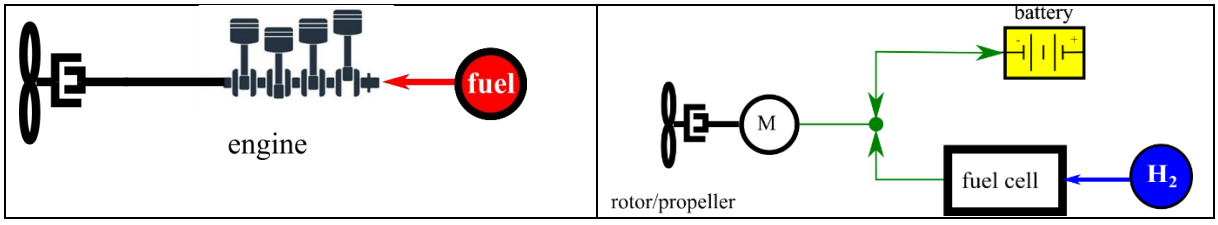

Figure 2. Original (left) and proposed (right) power systems

The original and proposed power systems, consisting of a lithium battery, a PEM fuel cell, and a compressed hydrogen vessel are depicted in Figure 2. The coupling between these components requires a certain number of electronic devices whose contribution to mass and volume is neglected in this

preliminary analysis. In the retrofitting, the mass of the new powertrain must be controlled not to exceed the max gross weight. To this scope, a total mass of 200kg is assumed as a target. As for the space constraint, an analysis of the space available in the aircraft led to the choice of a target value of 200L for the whole system.

2.1. Reference missions

Five missions named #01 #02, .,. , and #5 with a total flight time of 90 minutes were considered. They differ for cruise speed, propeller pitch setting, altitude, and climb rate but the details are not reported here for the sake of brevity. Each mission consists of six phases: takeoff, climb 1, cruise 1, climb 2, cruise 2, and descent. Two BLDC motors with a peak power of 124kW, a continuous power of 75kW, and a max speed of 6500rpm were selected. The motors are lighter and more compact than the original engine and present an efficiency higher than 94% in a large part of the torque/speed map.

By applying the basic laws of flight dynamics and taking into account the efficiency of the propeller and motor, and the power absorbed by the on-board services, the power profiles of Figure 3 are obtained for each phase of the missions.

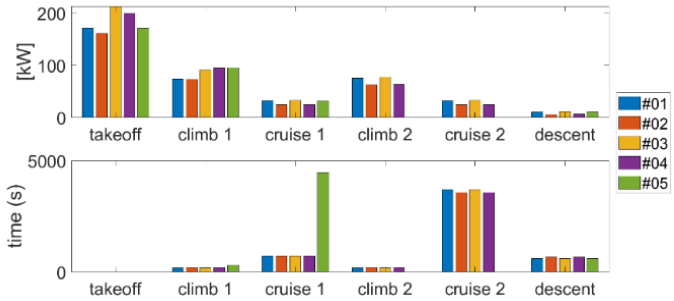

Figure 3. Requests of power in the six phases of the missions

3. Sizing methodology

The proposed methodology for the minimization of weight and volume of the power system (Figure 2b) consists of three steps and is illustrated in Figure 4. The design variable for the optimization is the fuel cell contribution to the takeoff power of the mission. This variable is called x_{FC} and is varied between 0 (battery-only configuration) to 100% (fuel cell-only configuration):

$$x_{FC} = \frac{P_{FC}}{P_{takeoff}} \cdot 100 \tag{1}$$

Where P_{FC} is the nominal power of the fuel cell and $P_{takeoff}$ is the electric power required by the electric motor during takeoff (which is the most demanding phase of the flight). The volume and mass of the whole power system is calculated for each value of x_{FC} as:

$$M(x_{FC}) = M_{batt}(x_{FC}) + M_{FC}(x_{FC}) + M_{H_2tank}(x_{FC}) \tag{2}$$

The volume is:

$$V(x_{FC}) = V_{batt} + V_{FC} + V_{H_2tank} \tag{3}$$

Before explaining the method used for the battery, we must recall the energy and the power that the battery can produce according to its nominal specification (capacity, voltage, and c-rate).

The energy made available by the battery is given by:

$$E_{batt} = DOD \cdot C_{nom} \cdot V_{batt} \tag{4}$$

The maximum continuous battery power can computed as:

$$P_{batt,max} = I_{max,dis} \cdot V = C_{rate,dis} \cdot C_{nom} \cdot V_{batt} \tag{5}$$

The battery current needs to be limited to avoid deterioration and damage. The maximum current in discharge, $I_{max,dis}$, and charge, $I_{max,ch}$, are expressed as multiples of the nominal capacity C_{nom}

$$I_{max,dis} = C_{rate,dis} \cdot C_{nom} \quad (6)$$

$$I_{max,ch} = C_{rate,ch} \cdot C_{nom} \quad (7)$$

Where $C_{rate,dis}$ and $C_{rate,ch}$ are battery specifications usually reported in the datasheets.

Like the motors, the battery can be discharged, for a short time, at a current larger than $I_{max,dis}$ that is named "burst current". However, this operating mode is not adopted here.

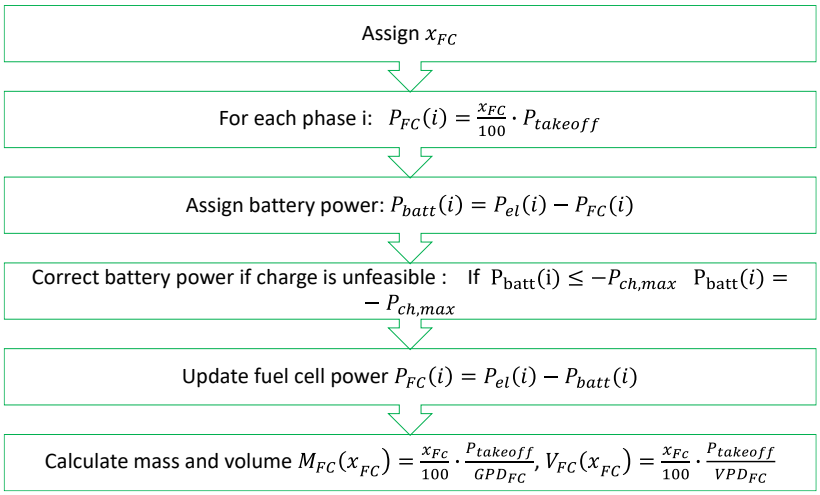

STEP 1: the fuel cell

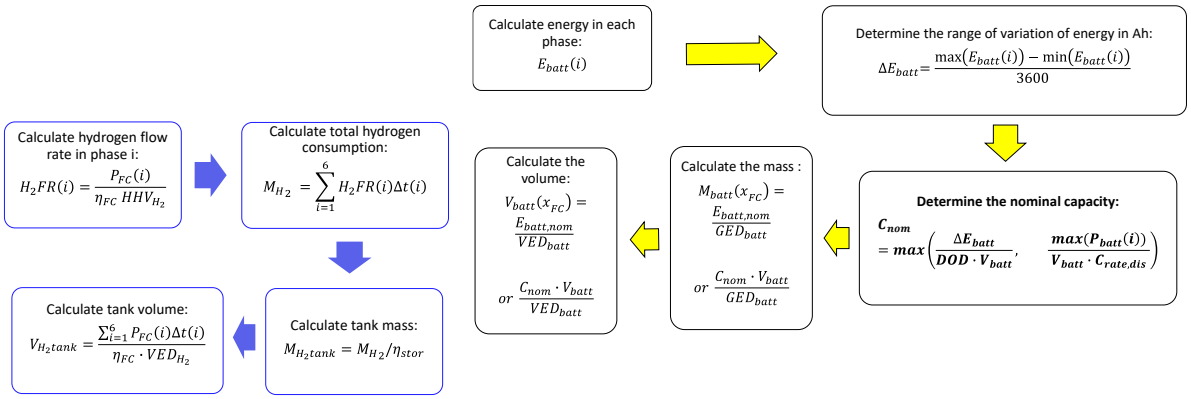

STEP 2: the hydrogen vessel STEP 3: the battery

Figure 4. Flow chart of the sizing methodology

The fuel cell mass and volume are calculated from preassigned values of the gravimetric power density (GPD) and volumetric power density (VGP). Two different energy management strategies are taken into account. In the first strategy, named "with charge", the fuel cell works at constant power during the whole flight. The battery is charged if the fuel cell power exceeds the request of electricity, provided that the charge power is compatible with the charging limits of the battery. Otherwise, the battery power (negative in our convention) is set equal to the maximum charging power ($P_{batt,ch}(i) = -I_{max,ch}V_{batt}$), and the fuel cell power is adjusted to match the electric power request. This check is performed at each phase of the flight. In the second strategy, "w/o charge", the procedure is the same but the maximum charging power is assumed equal to zero, so the battery cannot be charged during the flight. Therefore, in this second strategy, the load of the fuel cell is equal to the power request in the low-power flight segments. In the equations of Figure 4, η_{FC} is the average efficiency of the fuel cell

and HHV_{H_2} is the heating value of hydrogen. The mass of hydrogen is used to define the mass of the hydrogen tank through the storing efficiency η_{stor}.

The range of variation of battery energy, ΔE_{batt}, used to size the battery is explained in Figure 5. Since the battery can deliver only a percentage DOD (Depth of Discharge) of its nominal energy, the initial value of the nominal size of the battery in Wh is calculated by dividing the ΔE_{batt} by the desired DOD.

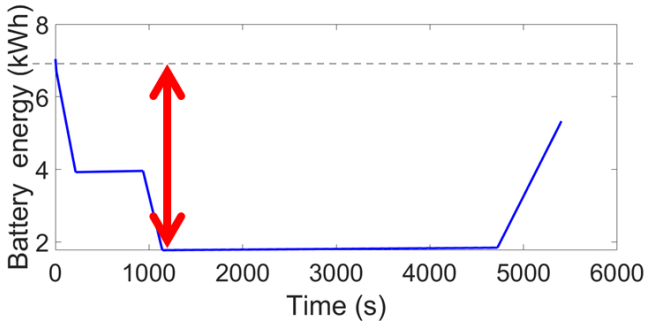

Figure 5. Typical battery energy trend if the battery can be charged during the low power phases of the flight. The red arrow indicates the range ΔE_{batt} used to size the battery.

However, this procedure is not sufficient to size the battery. As already explained, it is necessary to verify that $-P_{ch,max} \leq P_{batt}(i) \leq P_{dis,max}$. Therefore, the following constraints are to be met:

$$I_{max,batt}(i) = \frac{P_{dis,max}}{V_{batt} \cdot C_{nom}} = \frac{P_{batt}(1)}{V_{batt} \cdot C_{nom}} \leq C_{rate,dis} \cdot \tag{8}$$

$$\left|I_{min,batt}(i)\right| = \frac{\left|P_{ch,max}\right|}{V_{batt} \cdot C_{nom}} = \frac{|P_{batt}(6)|}{V_{batt} \cdot C_{nom}} \leq C_{rate,ch} \cdot \tag{9}$$

Table 1. List of the parameters assumed in the investigation and their values

	Variable	Description	Value	Source
Fuel cell	$\boldsymbol{GPD_{FC}}$	Gravimetric power density of the fuel cell	300 W/kg	Arco Fuel Cells datasheets
	$\boldsymbol{VPD_{FC}}$	Volumetric power density of the fuel cell	210 kW/L	Arco Fuel Cells, datasheets
	$\boldsymbol{\eta_{FC}}$	Fuel cell efficiency	45%	Arco Fuel Cells Datasheets, [12]
Hydrogen vessel	$\boldsymbol{HHV_{H_2}}$	Higher Heating Value of hydrogen	39000 Wh/kg	[15]
	$\boldsymbol{\eta_{stor}}$	Hydrogen storage efficiency (pressurized tank at 700bar)	5.5% ,	[3], [8]
	$\boldsymbol{VED_{H_2}}$	Volumetric energy density of compressed hydrogen at 700bar	1300 Wh/L (40kg/m^3)	[3] [16]
Battery	$\boldsymbol{DOD}$	Depth of discharge of the battery	75%	[8]
	$\boldsymbol{V_{batt}}$	Battery nominal voltage	370 V	
	$\boldsymbol{C_{rate,dis}}$	Battery c-rate for discharging	20	[8]
	$\boldsymbol{C_{rate,ch}}$	Battery c-rate for charging	0 and 5	
	$\boldsymbol{GED_{batt}}$	Gravimetric energy density of the battery	200 Wh/kg	[3]
	$\boldsymbol{VED_{batt}}$	Volumetric energy density of the battery	400 Wh/L	[17]

Therefore, the nominal capacity of the battery is selected by considering the more stringent requirement which, according to the value of x_{FC} can be either the energy demand or the power request.

After this check, the mass and the space occupied by the battery can be finally calculated by using appropriate values of the gravimetric (GED_{batt}) and volumetric (VED_{batt}) energy density, respectively. To solve the optimization problem, a full space exploration was adopted by varying x_{FC} between 0 and 100 with a step of 0.01 Thanks to the limited calculation time of the proposed procedure, faster optimization procedures were not contemplated.

3.1. Technological scenario

The proposed methodology includes several arbitrarily selected parameters that are summarized in Table 1, together with the values assumed in this investigation and their reference.

The family of lithium batteries is quite vast and, consequently, battery specifications like energy density, $C_{rate,dis}$, and $C_{rate,ch}$ have a large range of variation [9]. Actually, there is a trade-off between energy density and maximum battery power/current, so batteries designed to achieve very high values of energy density are characterized by limited discharging currents and consequently, low power density ([14], [7]). In this investigation, lithium polymer batteries are adopted. A future study could analyze the results of the method by accounting for the effect of $C_{rate,dis}$ on GPD_{FC} after acquiring a significant database of commercial batteries to model such dependence. In this investigation the max current of the battery was calculated with $C_{rate,dis} = 5$.

4. Results

The results of the methods for the long missions are discussed here for the two strategies, with and without battery charging.

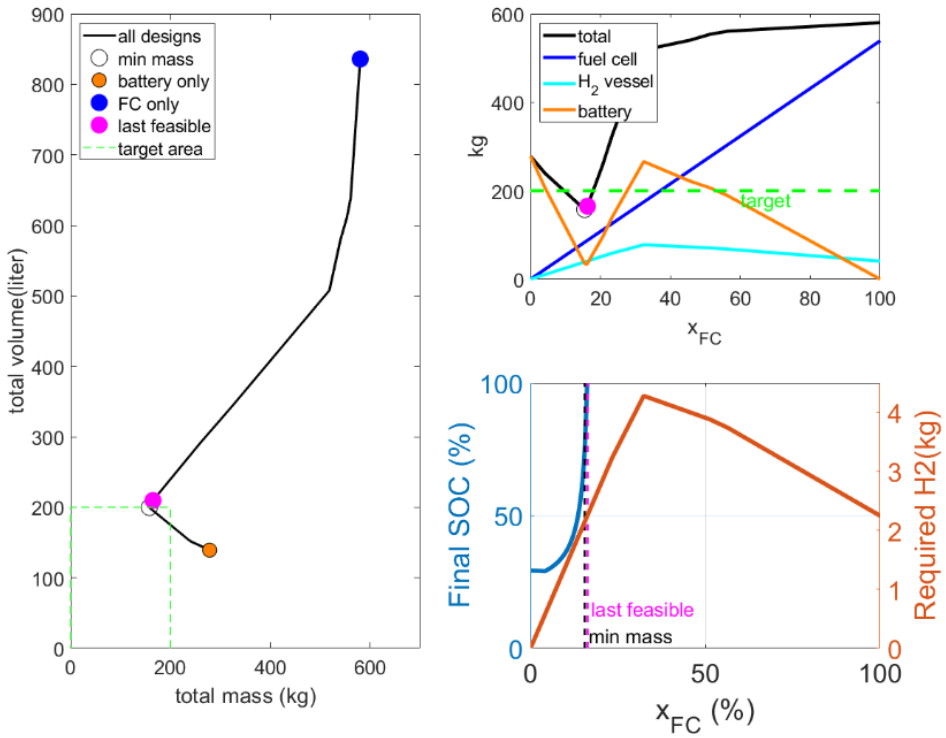

Figure 6. Results of the methodology for long mission #02 with battery charge at 5C

The plots of Figure 6 shows the results of the application of the methodology for mission #02 when the fuel cell is allowed to charge the battery with a current up to 5C. Similar results are obtained for the other missions. The plot at the right represents the globality of the design considered in the optimization

with x_{FC} that increases from zero (orange bubble) to 100 (blue bubble). Discontinuities in the black line are due to transition from battery sized for energy and battery sized for power and, in particular, to the saturation of the maximum charge current for the lower power phases (in the order descent, cruise1, cruise2, climb2). The two extremes represent the battery-only and the FC-only powertrains. Starting from the bottom (battery only), the mass of the hybrid electric configuration initially decreases with x_{FC} while the volume increases. This continues until reaching an optimum, named "*min mass*", that corresponds to the lowest mass configuration compatible with the selected mission. This solution can be accepted if it falls within the target area outlined by the dotted green line. A further increase in x_{FC} determines an increase in both mass and occupied space. The details of the mass contributions are reported in the plot at the top right of Figure 6. Note that the mass of the fuel cell is the most relevant for x_{FC}>13% because of its limited power density, while the battery is the critical component for x_{FC}<13%. The bottom right of Figure 6 shows the consumption of the hydrogen and the final state of charge of the battery for all designs. In the case of *min mass* configuration, the final state of charge is 75%, while in the *last feasible* configuration, the battery is fully charged at the end of the mission, and no external charge is required. This configuration requires a slightly higher volume and mass than the min mass configuration. Once the *last feasible* configuration is reached, a further increase in the fuel cell contribution x_{FC}, corresponds to a battery that is partially discharged at the beginning of the mission and fully charged at the end. This means that part of the hydrogen energy is stored in electricity form. This kind of behavior is considered *unfeasible*.

The results obtained for the other missions are similar and summarized in Table 2. The targets of total volume and mass are strictly satisfied only for mission #02.

Table 2. *Min mass* configuration with battery charge at 5C for missions #01 - #05

	mass (kg)	tot vol (L)	FC power (kW)	FC power (% of TO/cruise Power)	Battery Energy (kWh)
#01	193.3	253	32.4	18.8% / 99%	7.0
#02	157.7	199.5	25.1	15.5% / 100%	7.1
#03	203.8	258.4	32.4	15.2 / 97%	9.06
#04	169.3	207.9	25.5	12.8 / 100%	8.8
#05	197.4	253.7	32.1	18.7/100%	8.1

In the case without charge, the last feasible solution corresponds to the battery being used only at takeoff, while the rest of the mission is performed by using the fuel cell only. The *min mass* configuration is the same as found in the previous cases in terms of fuel cell and battery, while the hydrogen vessel is smaller because the battery needs not to be charged. This determines a reduction of mass and occupied space compared with the previous case *"with charge"*.

5. Conclusions

A methodology has been developed to minimize the volume and the mass of the power system at constant take-off mass over different operating missions. The fuel cell power working point was kept constant throughout the mission when compatible with the battery technological limits. The procedure was applied to the retrofitting of ultralight aircraft with on the market products for battery, fuel cell, and hydrogen vessel to minimize direct and indirect emissions of greenhouse gases. The results showed that for the proposed 90-minute missions, the adoption of the hybrid electric power system determines a very reduction of the weight by 44% compared with a battery-only configuration. The space occupied by the fuel cell was found to be particularly critical and the target of an overall volume below 200L was the most difficult to meet with the hybrid configuration. The results of this investigation will be used to develop a modular configuration for the 25kW fuel cell/ 7kWh battery that meets the targets for mission #02. A multi-stack configuration will be considered to ensure sufficient remaining power in case of

failure of one or two stacks. Moreover, the use of a modular configuration allows the deactivation of one or more stacks during the low-power phases of the flight. As a further investigation, the methodology will also be improved by taking into consideration the loss of power of the fuel cell system at high altitude and by considering different energy management strategies for the fuel cell.

6. Acknowledgments

This investigation is part of the project "Sviluppo di architetture propulsive ad emissioni zero per l'Aviazione generale (SERENA - CUP: F89J22003510004)", funded by the Italian Ministry for the Environment and Energy Security (MASE), M2-C2-I3.5 call of the Italian Recovery and Resilience Plan. The authors wish to thank the other partners of the project (DTA-Scarl and EngineSoft s.p.a.) for their valuable suggestions and helpful support.

7. References

[1] Sparano M, Sorrentino M, Troiano G, Cerino G, Piscopo G, Basaglia M, Pianese C 2023 *Energy Conversion and Management*, **281**, 116822.
[2] Ayar M, Karakoc T 2023 *International Journal of Hydrogen Energy* **48**, pp 23156-23167
[3] Geliev A V, Varyukhin A N, Zakharchenko V S, Kiselev I O, Zhuravlev D I 2019 *Proceedings of 2019 International Conference on Electrotechnical Complexes and Systems* ICOECS (Moscow: IEEE), p **1-17**.
[4] Romeo G, Cestino E, Correa G, Borello F 2011 *SAE International Journal of Aerospace*, **4** (2011-01-2522), 724-737
[5] Thomas C E 2009 *International Journal of Hydrogen Energy* **34** (15), 6005-6020
[6] Park J, Lee D, Yee K 2022 *AIAA AVIATION 2022 Forum* (Chicago: AIAA) p. 3514
[7] Miazga, T, Iwański G, Nikoniuk M 2021 *Energies* **14** (4), 1073
[8] Jarry T, Lacressonnière F, Jaafar A, Turpin C, Scohy M 2021 *Energies* **14** (22) 7655.
[9] Jarry T, Lacressonnière F, Jaafar A, Turpin C, Scohy M 2021 *Proceedings of 2021 International Conference on Electrical Computer and Energy Technologies* (Cape Town: IEEE) pp. 1-6.
[10] Nicolay S, Karpuk S, Liu Y, Elham A 2021 *International Journal of Hydrogen Energy* **46** (64), 32676-32694.
[11] Ayar M, Karakoc T H 2023 *International Journal of Hydrogen Energy* **48** p 23156 -23167
[12] Kasim A A, Marek E J 2022 *Journal of Power Sources* **521** 230987
[13] Donateo T, Çinar H 2022 *Journal of Physics: Conference Series* **2385**(1),012072
[14] Donateo T, Spedicato L 2017 A*pplied energy* **206** 230987 p 723-738
[15] Rubio F, Llopis-Albert C, Besa A J 2023 *Technological Forecasting and Social Change*, **188**, 122290
[16] Taccani R, Malabotti S, Dall'Armi C, Micheli D 2020 *International Shipbuilding Progress* **67** (1) p 33-56
[17] Muralidharan N, Self E C, Dixit M, Nanda J, Belharouak J 2022, *Advanced Energy Materials* **9 (**12)